Steroids xxx (2015) xxx–xxx

Contents lists available at ScienceDirect

Steroids

journal homepage: www.elsevier.com/locate/steroids

Molecular decodification of gymnemic acids from *Gymnema sylvestre*. Discovery of a new class of liver X receptor antagonists

Barbara Renga [a], Carmen Festa [b], Simona De Marino [b], Simone Di Micco [c], Maria Valeria D'Auria [b], Giuseppe Bifulco [c], Stefano Fiorucci [a], Angela Zampella [b,*]

[a] Department of Surgery and Biomedical Sciences, Nuova Facoltà di Medicina, P.zza L. Severi, 1-06132 Perugia, Italy
[b] Department of Pharmacy, University of Naples "Federico II", Via D. Montesano, 49, I-80131 Naples, Italy
[c] Department of Pharmacy, University of Salerno, Via Giovanni Paolo II, 132, 84084 Fisciano (Salerno), Italy

ARTICLE INFO

Article history:
Received 12 November 2014
Received in revised form 19 December 2014
Accepted 29 January 2015
Available online xxxx

Keywords:
Gymnemic acids
Gymnema sylvestre
Steroid nuclear receptors
Liver-X-receptor

ABSTRACT

The individual chemical components of commercial extract of *Gymnema sylvestre*, a medicinal plant used in the traditional systems of the Indian medicine for its antidiabetic and hypolipidemic properties, were isolated and evaluated for their capability to act as modulators of nuclear and membrane receptors involved in glucose and lipid homeostasis.

The study disclosed for the first time that individual gymnemic acids are potent and selective antagonists for the β isoform of LXR. Indeed the above activity was shared by the most abundant aglycone gymnemagenin (**10**) whereas gymnestrogenin (**11**) was endowed with a dual LXRα/β antagonistic profile. Deep pharmacological investigation demonstrated that gymnestrogenin, reducing the expression of SREBP1c and ABCA1 in vitro, is able to decrease lipid accumulation in HepG2 cells. The results of this study substantiate the use of *G. sylvestre* extract in LXR mediated dislypidemic diseases.

1. Introduction

Gymnema sylvestre (family Asclepiadaceae), known as "gurmar" (sugar destroyer) in Hindi, is a well-known plant native to central and western India that also grows wild in the tropical forests of Africa, Australia, and China. It is considered a relevant medicinal plant and is used since thousands of years in folk medicine and Ayurveda [1], especially for its antidiabetic properties, but also for the treatment of a broad range of ailments including asthma, eye complaints, family planning, colic pain, cardiopathy, constipation, dyspepsia, hemorrhoids, and hyperlipidemic conditions [2–5]. Several preclinical studies on polar/nonpolar extracts of roots and leaves of *G. sylvestre* suggested that *G. sylvestre* exerts its hypoglycemic effects through the increase in insulin secretion [6], in regeneration of islets cells [7], peripheral utilization of glucose and inhibition of glucose absorption from intestine. Further, clinical reports validated the use of *G. sylvestre* in type 1 and 2 diabetic conditions [8]. From a chemical point of view, *G. sylvestre* extracts contain triterpene saponins belonging to oleanane and dammarane classes [9,10]. Gymnemic acids (GAs), a complex mixture of oleanane saponins, are largely considered the active constituents, and the quality of extracts and its formulations is assessed by the content of gymnemic acids [11]. Besides several efforts have been reported on the beneficial effects of gymnemic acid crude extracts in ameliorating metabolic diseases, few reports on the effects of a single, structural characterized biological molecule have been published and few data are today available on the biological targets involved in GAs beneficial effects. A recent report disclosed two components of *G. sylvestre* crude extracts, gymnemic acids V and XV, as potent inhibitors of sodium-dependent glucose transporter 1 (SGLT1), demonstrating for the first time the role of selected components of GAs in inhibiting electrogenic glucose uptake in the gastrointestinal tract [12].

Indeed the varied pharmacological activities exhibited by *G. sylvestre* extracts in regulating body weight [13], lipid [14] and

Abbreviations: ABCA1, ATP-binding cassette transporter A1; (ABC)G1, ATP-binding cassette sub-family G member 1; apoE, apolipoprotein; CDCA, chenodeoxycholic acid; DCCC, droplet-counter-current-chromatography; FXR, farnesoid-X-receptor; GAs, gymnemic acids; LXR, liver X receptor; GP-BAR1, G protein-coupled bile acid receptor 1; HEK-293T, human embryonic kidney 293 cells; HepG2, human hepatoma cell line; LBD, ligand binding domain; PPARγ, peroxisome proliferator-activated receptor γ; PXR, pregnane-X-receptor; RXR, retinoid X receptor; SGLT1, sodium-dependent glucose transporter 1; SREBP-1c, sterol regulatory element-binding protein; TGs, plasma triglycerides; TLCA, taurolithocolic acid.

* Corresponding author. Tel.: +39 081 678525; fax: +39 081 678552.
E-mail address: angela.zampella@unina.it (A. Zampella).

http://dx.doi.org/10.1016/j.steroids.2015.01.024
0039-128X/

glucose homeostasis would suggest a modulation of liver X receptors (LXRs), transcriptional factors belonging to the superfamily of metabolic nuclear receptors.

Liver X receptor-α (LXRα) and liver X receptor-β (LXRβ) (also known as NR1H3 and NR1H2, respectively) are critical modulators of lipid and glucose metabolism, inflammatory responses and innate immunity. LXRs are ligand-activated transcription factors belonging to the nuclear receptor superfamily that controls biological responses by coordinating regulation of gene transcription [15–17]. As ligand-activated transcription factors, these receptors are amenable to modulation by small drug-like molecules, and LXRs have emerged as potential therapeutic targets for atherosclerosis, Alzheimer's disease and type 2 diabetes. The LXRs function as heterodimers with the retinoid X receptor (RXR) and are activated by naturally occurring cholesterol metabolites known as sterols and oxysterols [18,19]. Consistent with their role as sensors of cholesterol level, LXRs coordinately regulate set of genes to control cholesterol metabolism in various tissues [15,16]. In the liver, LXRα directly induces Cyp7a1, the rate-limiting enzyme in the classical bile acid biosynthesis pathway, leading to the catabolism of cholesterol to bile acids. In macrophages, adipocytes and other peripheral cell types, LXRs respond to high intracellular sterol levels by inducing cholesterol efflux through stimulation of expression of ATP-binding cassette ABCA1, (ABC)G1 and apolipoprotein (apoE) – proteins that increase the removal of excess cholesterol from cells [20–24]. In addition LXRs also participate in both innate and acquired immune responses [25,26], improve glucose tolerance and insulin sensitivity in both mouse and rat models of diabetes [27] through coordinate regulation of glucose metabolism in liver and adipose tissue [28]. As a consequence, LXRs agonists are recognized a promising strategy in the treatment of several human diseases including hypercholesterolemia, diabetes, autoimmune disorders, and neurodegenerative diseases [29].

In addition to their central role in cholesterol homeostasis, LXRs are important regulators of hepatic lipogenesis [30–32]. Indeed LXRs stimulate the expression of sterol regulatory element-binding protein (SREBP)-1c, acetyl-CoA carboxylase, stearoyl-CoA desaturase-1 and fatty acid synthase in the liver leading to increased fatty acid biosynthesis and plasma triglycerides (TGs). While LXRα and LXRβ are capable of inducing hepatic lipogenesis, studies in LXR knockout mice suggest that LXRα is the dominant isoform in this pathway [31]. A number of LXR agonists have been shown to induce hypertriglyceridemia and hepatic steatosis, and this observation hinders the development of this class of compounds for human use in atherosclerotic cardiovascular disease [33]. Indeed several recent efforts have demonstrated the utility of LXRs antagonists in human diseases in which hepatic fatty acid level are impaired. Fatty liver accumulation, which often accompanies obesity and type 2 diabetes, frequently leads to a much more debilitating hepatic disease including non-alcoholic steatohepatitis, cirrhosis, and hepatocellular carcinoma [34,35].

With this background in mind and within our long-standing interest in nuclear receptor modulators from natural sources [36,37], we proceeded in the isolation of individual gymnemic acids from a commercial available preparation of *G. sylvestre* extracts. Gymnemic acids **1**–**9** and the corresponding aglycone moieties gymnemagenin **10** and gymnestrogenin **11** (Fig. 1) were tested on a panel of metabolic nuclear receptors demonstrating for the first time their ability to antagonize LXRs. In detail, apart compound **2**, all isolated gymnemic acids as well as the most abundant aglycone gymnemagenin (**10**) were demonstrated potent and selective antagonists for LXRβ whereas gymnestrogenin (**11**) was endowed with a dual LXRα/β antagonistic profile.

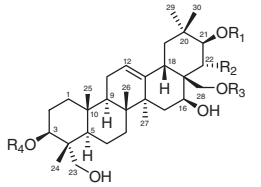

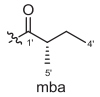

	R_1	R_2	R_3	R_4
Gymnemic acid VII (**1**)	H	H	H	GlcA
Gymnemagenin 3-O-glucuronide (**2**)	H	OH	H	GlcA
Gymnemic acid I (**3**)	tig	OH	Ac	GlcA
Gymnemic acid II (**4**)	mba	OH	Ac	GlcA
Gymnemic acid III (**5**)	mba	OH	H	GlcA
Gymnemic acid IV (**6**)	tig	OH	H	GlcA
Gymnemic acid V (**7**)	tig	Otig	H	GlcA
Gymnemic acid VIII (**8**)	H	OH	mba	GlcA
Gymnemic acid XI (**9**)	tig	OH	tig	GlcA
Gymnemagenin (**10**)	H	OH	H	H
Gymnestrogenin (**11**)	H	H	H	H

Fig. 1. Gymnemic acids (GAs) isolated from *Gymnema sylvestre*; tig: tigloyl; mba: (*S*)-2-methylbutyroyl.

2. Experimental

2.1. General experimental procedures

High-resolution ESIMS spectra were performed with a Micromass QTOF Micromass spectrometer. ESIMS experiments were performed on an Applied Biosystem API 2000 triplequadrupole mass spectrometer.

NMR spectra were obtained on Varian Inova 500 and 700 NMR spectrometers (^{1}H at 500 and 700 MHz, ^{13}C at 125 and 175 MHz, respectively) equipped with a Sun hardware, δ (ppm), J in Hz, spectra referred to CHD_2OD as internal standard (δ_H = 3.31 and δ_C = 49.0 ppm). Spin multiplicities are given as s (singlet), br s (broad singlet), d (doublet), dd (double doublet) or m (multiplet).

Droplet counter current chromatography (DCCC) was performed on a DCC-A apparatus (Tokyo Rikakikai Co., Tokyo, Japan) equipped with 250 glass-columns (internal diameter 3 mm).

HPLC was performed using a Waters 510 pump equipped with Waters Rheodyne injector and a Waters 401 differential refractometer as detector.

Silica gel MN Kieselgel 60 (70–230 mesh) from Macherey–Nagel Company was used for column chromatography.

The purities of compounds were determined to be greater than 95% by HPLC, MS and NMR.

2.2. Separation of individual gymnemic acids

Dried and finely powdered extract of *G. sylvestre* (3.0 g) was chromatographed in two runs by DCCC using $CHCl_3$/MeOH/H_2O (7:13:8) in the ascending mode (the lower phase was the stationary phase), flow rate 8 ml/min; 4 ml fractions were collected. Fractions were monitored by TLC on SiO_2 with *n*-BuOH/AcOH/H_2O (60:15:25) as eluent and combined on the basis of their similar TLC retention factors.

Fraction 2 (220 mg) was purified by HPLC on a reverse phase Nucleodur 100-5 C18 (5 μm; 4.6 mm i.d. × 250 mm) column eluting in isocratic mode with MeOH/H_2O (45:55) (flow rate 1 mL/min) to give 1.8 mg of gymnemagenin 3-O-glucuronide[38] (**2**) (t_R = 2.4 min) and 2.4 mg of gymnemic acid VII [39] (**1**) (t_R = 4.2 min) (Table S2 in Supporting information).

Fraction 3 (160 mg) was purified by HPLC on a reverse phase Nucleodur 100-5 C18 (5 μm; 4.6 mm i.d. × 250 mm) column eluting in isocratic mode with MeOH/H_2O (1:1) (flow rate 1 mL/min) to afford 3.1 mg of gymnemic acid IV [40] (**6**) (t_R = 8.1 min), 3.7 mg of gymnemic acid II [40] (**4**) (t_R = 9.6 min), 5.4 mg of gymnemic acid I [40] (**3**) (t_R = 17.1 min), 1.6 mg of gymnemic acid III [40] (**5**)

(t_R = 19.5 min), 0.7 mg of gymnemic acid VIII [41] (**8**) (t_R = 21.3 min) (Table S2 in Supporting information).

Fraction 4 (60 mg) was purified by HPLC on a reverse phase Nucleodur 100-5 C18 (5 μm; 4.6 mm i.d. × 250 mm) column eluting in isocratic mode with MeOH/H_2O (65:35) (flow rate 1 mL/min) to give 1.6 mg of gymnemic acid V [38,39] (**7**) (t_R = 15.6 min) and 1.5 mg of gymnemic acid XI [41] (**9**) (t_R = 22.8 min) (Table S2 in Supporting information).

*2.2.1. Gymnemic acid VII (**1**)*

White amorphous solid; selected ^{1}H NMR (500 MHz, CD_3OD): 5.28 (1H, br s, H-12), 4.42 (1H, d, *J* = 7.9 Hz, H-1″), 4.20 (1H, dd, *J* = 11.8, 5.3 Hz, H-16), 3.75 (1H, d, *J* = 10.6 Hz, H-28a), 3.55 (1H, d, *J* = 10.8 Hz, H-23a), 3.32 (1H, overlapped with solvent signal, H-28b), 3.30 (1H, overlapped with solvent signal, H-23b), 2.27 (1H, dd, *J* = 13.5, 3.8 Hz, H-18), 1.25 (3H, s, H_3-27), 1.02 (3H, s, H_3-26), 1.00 (3H, s, H_3-25), 0.95 (3H, s, H_3-30), 0.88 (3H, s, H_3-29), 0.71 (3H, s, H_3-24). ESI-MS: *m*/*z* 665.4 [M−H]$^-$. HRMS (ESI): calcd. for $C_{36}H_{57}O_{11}$ 665.3901; found 665.3909 [M−H]$^-$.

*2.2.2. Gymnemagenin 3-O-glucuronide (**2**)*

White amorphous solid; selected ^{1}H NMR (500 MHz, CD_3OD): 5.35 (1H, br s, H-12), 4.60 (1H, dd, *J* = 11.0, 5.4 Hz, H-16), 4.43 (1H, d, *J* = 7.8 Hz, H-1″), 3.97 (1H, d, *J* = 10.4 Hz, H-22), 3.54 (1H, d, *J* = 10.4 Hz, H-21), 2.65 (1H, dd, *J* = 14.5, 4.1 Hz, H-18), 1.27 (3H, s, H_3-27), 1.02 (3H, s, H_3-25), 1.03 (3H, s, H_3-26), 0.99 (3H, s, H_3-30), 0.91 (3H, s, H_3-29), 0.71 (3H, s, H_3-24). ESI-MS: *m*/*z* 681.4 [M−H]$^-$. HRMS (ESI): calcd. for $C_{36}H_{57}O_{12}$ 681.3850; found 681.3852 [M−H]$^-$.

*2.2.3. Gymnemic acid I (**3**)*

White amorphous solid; selected ^{1}H NMR (500 MHz, CD_3OD): 6.91 (1H, q, *J* = 7.2 Hz, H-3′), 5.34 (1H, br s, H-12), 5.18 (1H, d, *J* = 10.7 Hz, H-21), 4.77 (1H, dd, *J* = 11.4, 5.5 Hz, H-16), 4.42 (1H, d, *J* = 7.6 Hz, H-1″), 4.34 (1H, d, *J* = 10.9 Hz, H-28a), 4.22 (1H, d, *J* = 10.9 Hz, H-28b), 4.07 (1H, d, *J* = 10.7 Hz, H-22), 2.63 (1H, dd, *J* = 13.7, 4.4 Hz, H-18), 2.09 (3H, s, $OCOCH_3$), 1.87 (3H, s, H_3-2′), 1.83 (3H, d, *J* = 7.2 Hz, H_3-4′), 1.31 (3H, s, H_3-27), 1.05 (3H, s, H_3-25), 1.02 (3H, s, H_3-26), 1.01 (3H, s, H_3-30), 0.88 (3H, s, H_3-29), 0.71 (3H, s, H_3-24). ESI-MS: *m*/*z* 805.4 [M−H]$^-$. HRMS (ESI): calcd. for $C_{43}H_{65}O_{14}$ 805.4374; found 805.4381 [M−H]$^-$.

*2.2.4. Gymnemic acid II (**4**)*

White amorphous solid; selected ^{1}H NMR (500 MHz, CD_3OD): 5.33 (1H, br s, H-12), 5.12 (1H, d, *J* = 10.7 Hz, H-21), 4.75 (1H, dd, *J* = 11.5, 5.0 Hz, H-16), 4.44 (1H, d, *J* = 7.7 Hz, H-1″), 4.33 (1H, *d*, *J* = 10.9 Hz, H-28a), 4.22 (1H, d, *J* = 10.9 Hz, H-28b), 4.03 (1H, d, *J* = 10.7 Hz, H-22), 2.63 (1H, dd, *J* = 14.2, 4.3 Hz, H-18), 2.48 (1H, m, H-2′), 2.10 (3H, s, $OCOCH_3$), 1.31 (3H, s, H_3-27), 1.18 (3H, d, *J* = 6.5 Hz, H_3-5′), 1.03 (3H, s, H_3-25), 1.02 (3H, s, H_3-26), 1.01 (3H, s, H_3-30), 0.96 (3H, t, *J* = 7.2 Hz, H_3-4′), 0.90 (3H, s, H_3-29), 0.72 (3H, s, H_3-24). ESI-MS: *m*/*z* 807.4 [M−H]$^-$. HRMS (ESI): calcd. for $C_{43}H_{67}O_{14}$ 807.4531; found 807.4540 [M−H]$^-$.

*2.2.5. Gymnemic acid III (**5**)*

White amorphous solid; selected ^{1}H NMR (500 MHz, CD_3OD): 5.37 (1H, br s, H-12), 5.10 (1H, d, *J* = 10.7 Hz, H-21), 4.70 (1H, dd, *J* = 11.4, 5.3 Hz, H-16), 4.42 (1H, d, *J* = 7.9 Hz, H-1″), 4.14 (1H, d, *J* = 10.7 Hz, H-22), 3.89 (1H, d, *J* = 10.6 Hz, H-28a), 3.57 (1H, ovl, H-28b), 2.71 (1H, dd, *J* = 13.9, 4.5 Hz, H-18), 2.47 (1H, m, H-2′), 1.30 (3H, s, H_3-27), 1.17 (3H, d, *J* = 6.8 Hz, H_3-5′), 1.03 (3H, s, H_3-25), 1.02 (3H, s, H_3-26), 1.00 (3H, s, H_3-30), 0.96 (3H, t, *J* = 7.6 Hz, H_3-4′), 0.88 (3H, s, H_3-29), 0.72 (3H, s, H_3-24). ESI-MS: *m*/*z* 765.4 [M−H]$^-$. HRMS (ESI): calcd. for $C_{41}H_{65}O_{13}$ 765.4425; found 765.4432 [M−H]$^-$.

*2.2.6. Gymnemic acid IV (**6**)*

White amorphous solid; selected ^{1}H NMR (500 MHz, CD_3OD): 6.91 (1H, q, *J* = 6.9 Hz, H-3′), 5.38 (1H, br s, H-12), 5.16 (1H, d, *J* = 10.7 Hz, H-21), 4.75 (1H, dd, *J* = 11.5, 5.0 Hz, H-16), 4.43 (1H, d, *J* = 7.8 Hz, H-1″), 4.18 (1H, d, *J* = 10.7 Hz, H-22), 3.90 (1H, d, *J* = 10.8 Hz, H-28a), 3.57 (1H, d, *J* = 10.8 Hz, H-28b), 2.70 (1H, dd, *J* = 14.0, 4.4 Hz, H-18), 1.87 (3H, s, H_3-2′), 1.82 (3H, d, *J* = 6.9 Hz, H_3-4′), 1.31 (3H, s, H_3-27), 1.04 (3H, s, H_3-25), 1.03 (3H, s, H_3-26), 1.02 (3H, s, H_3-30), 0.86 (3H, s, H_3-29), 0.71 (3H, s, H_3-24). ESI-MS: *m*/*z* 763.4 [M−H]$^-$. HRMS (ESI): calcd. for $C_{41}H_{63}O_{13}$ 763.4269; found 763.4275 [M−H]$^-$.

*2.2.7. Gymnemic acid V (**7**)*

White amorphous solid; selected ^{1}H NMR (500 MHz, CD_3OD): 6.78 (2H, m, H-3′ and H-3″), 5.62 (1H, d, *J* = 11.2 Hz, H-21 or H-22), 5.41 (1H, br s, H-12), 5.30 (1H, d, *J* = 11.2 Hz, H-21 or H-22), 4.72 (1H, dd, *J* = 11.5, 5.0 Hz, H-16), 4.43 (1H, d, *J* = 7.8 Hz, H-1″), 2.73 (1H, dd, *J* = 14.3, 4.0 Hz, H-18), 1.87 (6H, s, H_3-2′ and H_3-2″), 1.85 (6H, ovl, H_3-4′ and H_3-4″), 1.31 (3H, s, H_3-27), 1.04 (3H, s, H_3-25), 1.03 (3H, s, H_3-26), 1.02 (3H, s, H_3-30), 0.86 (3H, s, H_3-29), 0.71 (3H, s, H_3-24). ESI-MS: *m*/*z* 845.4 [M−H]$^-$. HRMS (ESI): calcd. for $C_{46}H_{69}O_{14}$ 845.4687; found 845.4693 [M−H]$^-$.

*2.2.8. Gymnemic acid VIII (**8**)*

White amorphous solid; selected ^{1}H NMR (500 MHz, CD_3OD): 5.28 (1H, br s, H-12), 4.67 (1H, dd, *J* = 11.3, 5.3 Hz, H-16), 4.42 (1H, d, *J* = 7.7 Hz, H-1″), 4.32 (1H, d, *J* = 10.8 Hz, H-28a), 4.22 (1H, d, *J* = 10.8 Hz, H-28b), 2.60 (1H, dd, *J* = 14.4, 4.6 Hz, H-18), 2.42 (1H, m, H-2′), 1.29 (3H, s, H_3-27), 1.18 (3H, d, *J* = 6.7 Hz, H_3-5′), 1.02 (3H, s, H_3-25), 1.01 (3H, s, H_3-26), 1.00 (3H, s, H_3-30), 0.92 (3H, t, *J* = 7.6 Hz, H_3-4′), 0.93 (3H, s, H_3-29), 0.71 (3H, s, H_3-24). ESI-MS: *m*/*z* 765.4 [M−H]$^-$. HRMS (ESI): calcd. for $C_{41}H_{65}O_{13}$ 765.4425; found 765.4433 [M−H]$^-$.

*2.2.9. Gymnemic acid XI (**9**)*

White amorphous solid; selected ^{1}H NMR (500 MHz, CD_3OD): 6.91 (2H, m, H-3′ and H-3″), 5.31 (1H, br s, H-12), 5.19 (1H, d, *J* = 10.6 Hz, H-21), 4.80 (1H, dd, *J* = 11.2, 5.0 Hz, H-16), 4.42 (1H, d, *J* = 7.8 Hz, H-1″), 4.40 (1H, d, *J* = 10.7 Hz, H-28a), 4.27 (1H, d, *J* = 10.7 Hz, H-28b), 4.10 (1H, d, *J* = 10.6 Hz, H-22), 2.67 (1H, dd, *J* = 14.2, 4.4 Hz, H-18), 1.84 (6H, s, H_3-2′ and H_3-2″), 1.82 (6H, ovl, H_3-4′ and H_3-4″), 1.32 (3H, s, H_3-27), 1.06 (3H, s, H_3-25), 1.03 (3H, s, H_3-26), 1.01 (3H, s, H_3-30), 0.89 (3H, s, H_3-29), 0.71 (3H, s, H_3-24). ESI-MS: *m*/*z* 845.4 [M−H]$^-$. HRMS (ESI): calcd. for $C_{46}H_{69}O_{14}$ 845.4687; found 845.4689 [M−H]$^-$.

2.3. Acid Hydrolysis of fraction 3

30 mg of fraction 3 from DCCC was dissolved in 5% H_2SO_4 in 50% MeOH (2 mL) and was heated at 100 °C for 2 h. The reaction mixture was neutralized with $NaHCO_3$ and evaporated to dryness to give a solid residue, that was purified by silica gel chromatography, eluting with $CHCl_3$/MeOH 9:1. The mixture (25 mg) was purified by HPLC on a Nucleodur 100–5 C18 (5 μm; 4.6 mm i.d. × 250 mm) with MeOH/H_2O (8:2) as eluent (flow rate 1 mL/min), to give 2.5 mg of gymnemagenin [38] (**10**) (t_R = 6 min) and 1.2 mg of gymnestrogenin [39] (**11**) (t_R = 8.4 min).

*2.3.1. Gymnemagenin (**10**)*

White amorphous solid; ^{1}H and ^{13}C NMR spectroscopic data in CD_3OD given in Supporting information, Table S1. ESI-MS: *m*/*z* 505.3 [M−H]$^-$. HRMS (ESI): calcd. for $C_{30}H_{49}O_6$ 505.3529; found 505.3533 [M−H]$^-$.

Please cite this article in press as: Renga B et al. Molecular decodification of gymnemic acids from *Gymnema sylvestre*. Discovery of a new class of liver X receptor antagonists. Steroids (2015), http://dx.doi.org/10.1016/j.steroids.2015.01.024

2.3.2. Gymnestrogenin (**11**)

White amorphous solid; ^{1}H and ^{13}C NMR spectroscopic data in CD_3OD given in Supporting information, Table S1. ESI-MS: *m/z* 489.3 $[M-H]^-$. HRMS (ESI): calcd. for $C_{30}H_{49}O_5$ 489.3580; found 489.3585 $[M-H]^-$.

2.4. Cell cultures

HepG2 cells were cultured in E-MEM supplemented with 10% FBS, 1% glutamine, 1% penicillin/streptomycin. THP-1 cells were cultured in RPM-I supplemented with 10% FBS, 2 mmol/L L-glutamine, 1% penicillin/streptomycin.

2.5. Transactivation assay

To investigate the LXRα and LXRβ mediated transactivation, HepG2 cells were plated at 5×10^4 cells/well in a 24 well plate. Cells were transfected with 200 ng reporter vector $p(UAS)_{5X}$TKLuc, 100 ng of a vector containing the ligand binding domain of LXRα or LXRβ cloned upstream of the GAL4-DNA binding domain (i.e. pSG5-LXRαLBD-GAL4DBD or pSG5-LXRβLBD-GAL4DBD) and 100 of pGL4.70 (Promega), a vector encoding the human Renilla gene.

To investigate the specificity of compounds **1**–**11** versus PPARγ, HepG2 cells were transiently transfected with 200 ng reporter vector $p(UAS)_{5X}$TKLuc, 100 ng pGL4.70 and with a vector containing the ligand binding domain of nuclear receptors PPARγ cloned upstream of the GAL4-DNA binding domain (pSG5-PPARγLBD-GAL4DBD).

To investigate the specificity of compounds **1**–**11** versus PXR, HepG2 cells were transfected with 100 ng pSG5-PXR, 100 ng pSG5-RXR, 100 ng pGL4.70 and with 200 ng of the reporter vector containing the PXR target gene promoter (CYP3A4 gene promoter) cloned upstream of the luciferase gene (pCYP3A4promoter-TKLuc).

To investigate the specificity of compounds **1**–**11** versus FXR, HepG2 cells were transfected with 200 ng of the reporter vector p(hsp27)-TK-LUC containing the FXR response element IR1 cloned from the promoter of heat shock protein 27 (hsp27), 100 ng of pSG5-FXR, 100 ng of pSG5-RXR, and 100 of pGL4.70 (Promega), a vector encoding the human Renilla gene.

To investigate the specificity of compounds **1**–**11** versus GP-BAR1, HEK-293T cells were plated at 1×10^4 cells/well in a 24 well-plate and transfected with 200 ng of pGL4.29 (Promega), a reporter vector containing a cAMP response element (CRE) that drives the transcription of the luciferase reporter gene luc2P, with 100 ng of pCMVSPORT6-human GP-BAR1, and with 100 ng of pGL4.70.

At 24 h post-transfection, cells were stimulated 18 h with 10 μM GW3965, a dual LXRα and β agonist, and compounds **1**–**11**. For dose–response curves, cells were transfected as described above and then treated with increasing concentrations of **11** (0.1, 1, 10, 25 μM). After treatments, 10 μL of cellular lysates were read using Dual Luciferase Reporter Assay System (Promega Italia s.r.l., Milan, Italy) according manufacturer specifications using the Glomax20/20 luminometer (Promega Italia s.r.l., Milan, Italy).

2.6. Real-Time PCR

Total RNA was isolated using the TRIzol reagent according to the manufacturer's specifications (Invitrogen). One μg RNA was purified of the genomic DNA by DNase I treatment (Invitrogen) and random reverse-transcribed with Superscript II (Invitrogen) in a 20 μL reaction volume. Ten ng template was added to the PCR mixture (final volume 25 μL) containing the following reagents: 0.2 μM of each primer and 12.5 μL of 2X SYBR FAST Universal ready mix (Invitrogen). All reactions were performed in triplicate and the thermal cycling conditions were: 2 min at 95 °C, followed by 40 cycles of 95 °C for 20 s, 60 °C for 30 s in iCycler iQ instrument (Biorad). The relative mRNA expression was calculated and expressed as $2^{-(\Delta\Delta Ct)}$. Forward and reverse primer sequences were the following: human GAPDH: GAAGGTG AAGGTCGGAGT and CATGGGTGGAATCATATTGGAA; human (SREBP)-1c: GCAAGGCCATCGACTACATT and GGTCAGTGTGTCCTCC ACCT; human ABCA1: GCTTGGGAAGATTTATGACAGG and AGGGGA TGATTGAAAGCAGTAA; human LXRα: CAACCCTGGGAGTGAGAGT ATC and ATAGCAATGAGCAAGGCAAACT; human LXRβ: AGGCATCC ACTATCGAGATCAT and GTCCTTGCTGTAGGTGAAGTCC.

2.7. ORO staining

HepG2 cells were grown at an initial density of 10^5 cells/well in a 6-well plate and treated daily for 7 d with 10 μM GW3965 or with the combination of GW3965 plus **11** (10 μM). Cells were then washed three times with iced PBS and fixed with 10% formalin for 60 min. After fixation, cells were washed with ddH_20, with 60% isopropanol for 5 min and then stained with Oil Red O working solution (obtained by mixing 6 mL Oil Red O stock solution (0.35 g Oil Red O powder dissolved in 100% isopropanol) with 4 mL ddH_20) for 15 min at room temperature. Cells were washed immediately 4 times with ddH_20 and acquired under microscope for qualitative analysis of Oil Red O accumulation. To quantify Oil Red O content levels, Oil Red O was eluted by incubating cells with 1 mL 100% isopropanol for 10 min with gently shaking. Density of samples were read at 500 nm on a spectrophotometer (Thermo) using 100% isopropanol as blank.

2.8. Computational details

The structures of **10** and **11** were built by the graphical interface Maestro 9.6 and their geometries optimized through MacroModel 10.2 software package [42] and using the MMFFs force field [43]. The geometries of both small molecules were optimized using the Polak–Ribier conjugate gradient algorithm (PRCG, 9×10^7 steps, maximum derivative less than 0.001 kcal/mol), using a GB/SA (generalized Born/surface area) [44] solvent treatment to mimic the presence of H_2O. The structures of isoforms α and β were downloaded from Protein Data Bank (www.rcsb.org) [45,46] with the PDB IDs: 3IPU [43] (LXRα) and 3L0E (LXRβ) [47] The macromolecules for the docking calculations were processed by Protein Preparation Wizard [48,49] module from Schrödinger suite 2013-3: ligand, water molecules and chains B, C and D were deleted; hydrogens and missing residues were added, the charges of side chains were assigned considering their pKa at physiological pH of 7.4. For Induced Fit Docking, we applied the extended protocol, producing 80 ligand–protein poses for both ligands with LXRα,β. The coordinates of co-crystal ligands with isoform α (PDB ID: 3IPU) and β (PDB ID: 3L0E) were used for grid generation. The conformational search was performed allowing the sample ring conformations of the ligands (**10** and **11**), with an energy window of 2.5 kcal/mol. For Prime refinement, the default values were used.

3. Results

Dried and finely powdered extract of *G. sylvestre* (3.0 g) was purified by DCCC ($CHCl_3$/MeOH/H_2O (7:13:8), ascending mode) followed by reverse-phase HPLC to afford gymnemic acid VII (**1**), gymnemagenin 3-O-glucuronide (**2**), gymnemic acids I–V (**3**–**7**), gymnemic acid VIII (**8**), and gymnemic acid XI (**9**). The chemical structures were identified by means of MS and 1D/2D-NMR experiments (see Experimental section and Supporting information). Comparison of all spectroscopic data with those previously reported in the literature [38–41] led to the unequivocal identification of

Please cite this article in press as: Renga B et al. Molecular decodification of gymnemic acids from *Gymnema sylvestre*. Discovery of a new class of liver X receptor antagonists. Steroids (2015), http://dx.doi.org/10.1016/j.steroids.2015.01.024

compounds **1**–**9** as reported in the Fig. 1. As shown, all gymnemic acids are triterpene glycosides invariably presenting at least one unit of D-glucuronic acid linked at C-3 hydroxyl group on the ring A of the aglycone moiety. Compounds **2**–**9** share the same aglycone unit identified in 3β,16β,21β,22α,23,28-hexahydroxyolean-12-ene, also known as gymnemagenin (**10**), whereas gymnemic acid VII (**1**), lacking the hydroxyl group at C-22 on ring E, is the corresponding 3-O-glucuronide of gymnestrogenin (**11**). Gymnemagenin (**10**) and gymnestrogenin (**11**) were obtained as pure samples through acid hydrolysis on the crude extract of *G. sylvestre* followed by careful HPLC separation. Apart compounds **1** and **2**, all isolated gymnemic acids possess one or two acylating units (acetyl, (*S*)-2-methylbutyroyl, tigloyl) involved in an ester bond with the hydroxyl group(s) on the aglycone ring E.

Gymnemic acids **1**–**9** and the corresponding aglycones **10**–**11** were first investigated for their ability to transactivate LXRα and LXRβ. As shown in Fig. 2A and C, we demonstrated that several compounds analyzed in this study were able to reduce the basal transactivation of both LXRα and LXRβ, respectively (Fig. 2A and C, $^{*}p < 0.05$ versus not treated cells). Furthermore, when compounds **1**–**11** were co-administered with GW3965 (a dual LXRα/β agonist), we observed that, except compound **2**, all gymnemic acids and the aglycones gymnemagenin (**10**) and gymnestrogenin (**11**) were potent antagonist for LXRβ (Fig. 2D, $^{\#}p < 0.05$ versus GW3965 administered cells). By the contrast, when **1**–**11** were tested on LXRα, we found that only gymnestrogenin (**11**) was able to antagonize the effect of GW3965 (Fig. 2B, $^{\#}p < 0.05$ versus GW3965 administered cells).

The relative antagonism potency of **11** was first investigated by a detailed measurement of concentration–response curve on LXRα and LXRβ transactivation. As illustrated in Fig. 3, gymnestrogenin (**11**) antagonized both LXRα and LXRβ transactivation with an IC_{50} of 2.5 and 1.4 μM, respectively.

To investigate the specificity of the above described compounds, we have tested whether compounds **1**–**11** interact with other metabolic nuclear receptors such as FXR, PXR and PPARγ and also with GP-BAR1, a membrane G-protein coupled receptor activated by endogenous bile acids and several natural occurring triterpenenoids [50]. Our investigations revealed that these compounds at the concentration of 10 μM failed to transactivate FXR, GP-BAR1, PXR and PPARγ (Fig. 4A–D).

Among all tested compounds, gymnestrogenin (**11**) represents promising template in generating selective dual LXRα/β antagonists. Thus, to further certificate that **11** specifically antagonizes LXRα and LXRβ we have investigated the possibility that **11** could antagonize other nuclear receptors including FXR, GP-BAR1, PXR

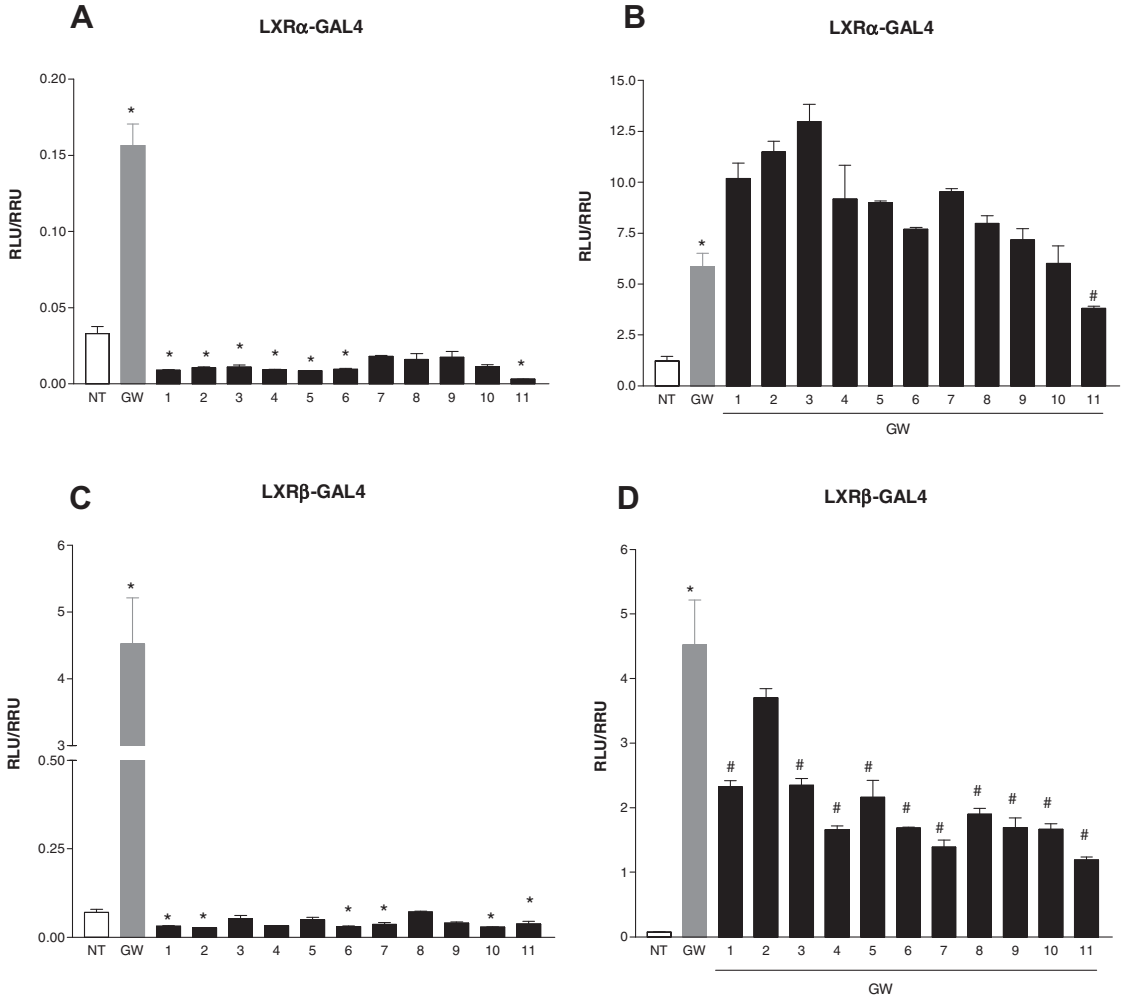

Fig. 2. Effect of gymnemic acids **1**–**9** and aglycones **10**–**11** on LXRs transactivation. (A-B) HepG2 cells were transiently transfected with a chimeric receptor plasmid in which the Gal4 DNA binding domain is fused to the LBD of LXRα (pSG5GAL4-LXRαLBD) and with the reporter vector $p(UAS)_{5x}$TKLuc. (C-D) HepG2 cells were transiently transfected with a chimeric receptor plasmid in which the Gal4 DNA binding domain is fused to the LBD of LXRβ (pSG5GAL4-LXRβLBD) and with the reporter vector $p(UAS)_{5x}$TKLuc. 24 h post transfection cells were stimulated for 18 h with GW3965 (10 μM), a dual LXRα/β agonist, with compounds **1**–**11** (10 μM) or with the combination of GW3965 (10 μM) plus compounds **1**–**11** (50 μM). Data are the mean ± S.E. of three experiments. $^{*}p < 0.05$ versus not treated cells (NT). $^{\#}p < 0.05$ versus GW3965 stimulated cells.

Please cite this article in press as: Renga B et al. Molecular decodification of gymnemic acids from *Gymnema sylvestre*. Discovery of a new class of liver X receptor antagonists. Steroids (2015), http://dx.doi.org/10.1016/j.steroids.2015.01.024

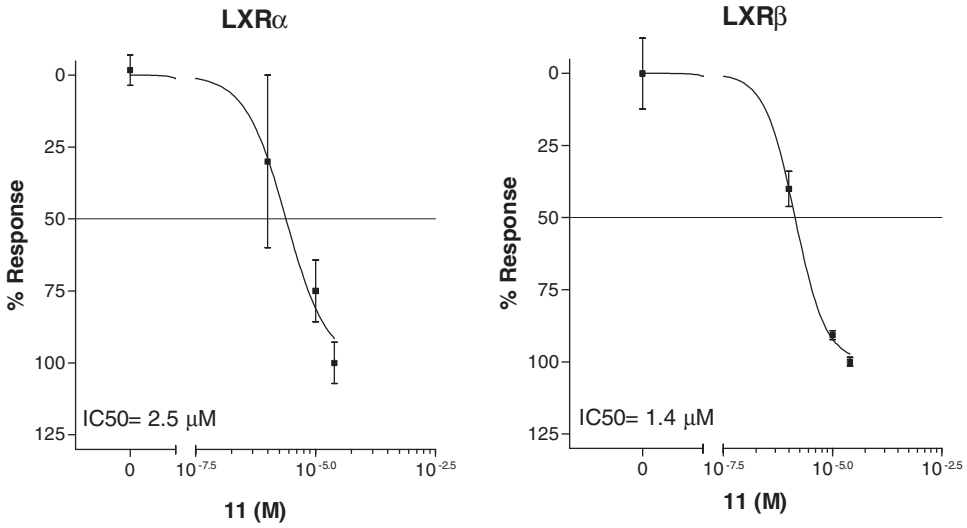

Fig. 3. Concentration–response curve of gymnestrogenin (**11**) on LXRα (A) and LXRβ (B). LXRα and LXRβ transacriptional activities were measured in HepG2 cells transfected using the GAL4-LBD fusion system. Twenty-four hour post transfection cells were stimulated with 10 μM GW3965, a dual LXRα/β agonist, in presence of increasing concentration of **11** (0.1, 1, 10 and 25 μM).

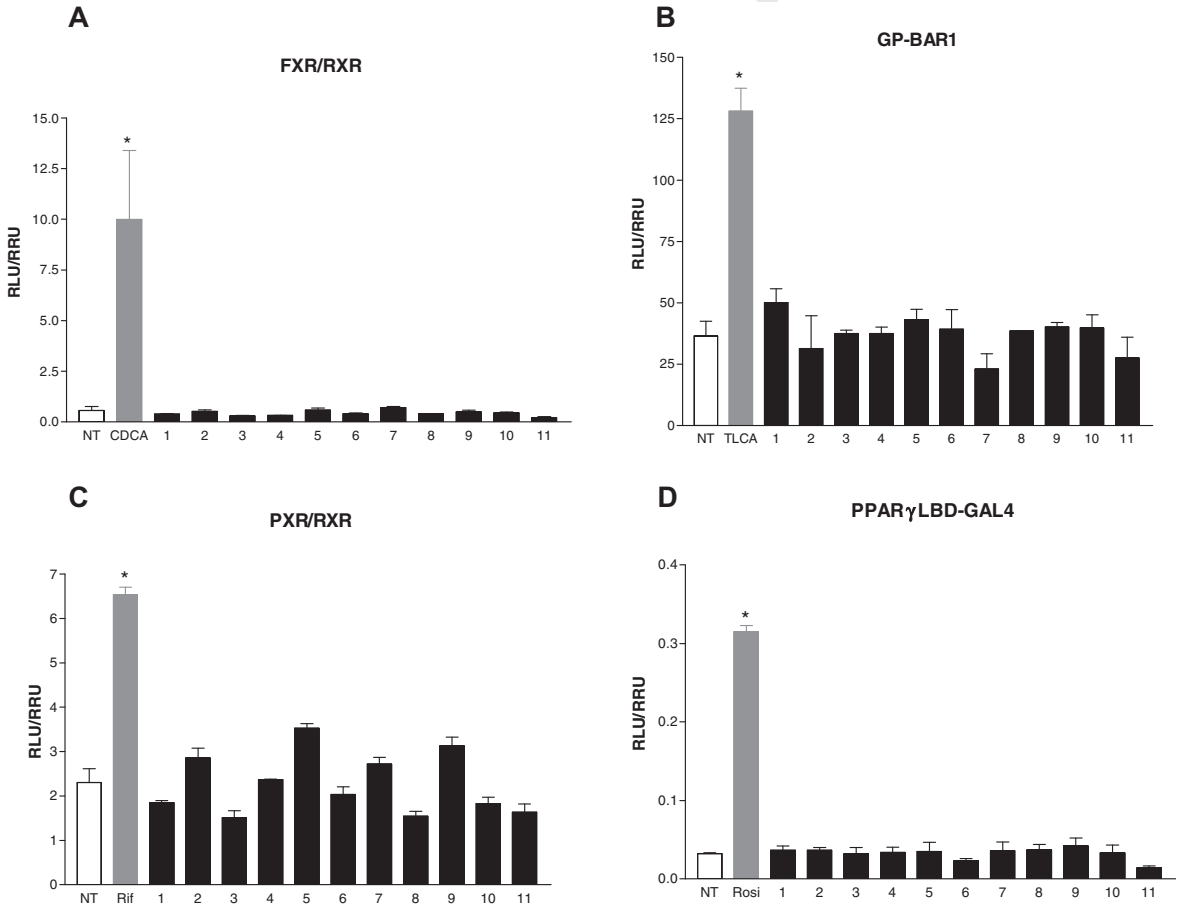

Fig. 4. Specificity of gymnemic acids **1**–**9** and the aglycones **10**–**11** on other nuclear receptors. (A) HepG2 cells were cotransfected with pSG5-FXR, pSG5-RXR, and with the reporter vector phsp27TKLuc and then stimulated 18 h with CDCA (10 μM), a FXR agonist, or with **1**–**11** (10 μM); (B) HEK293T cells were cotrasfected with pCMVSPORT-GP-BAR1 and with a reporter gene containing a cAMP responsive element in front of the luciferase gene (CRE) and stimulated 18 h with TLCA, (10 μM), a GP-BAR1 agonist, or with **1**–**11** (10 μM); (C) HepG2 cells were cotransfected with pSG5-PXR, pSG5-RXR, and with the reporter pCYP3A4 promoter-TKLuc and then stimulated 18 h with rifaximin (Rif, 10 μM), a PXR agonist, or with **1**–**11** (10 μM); (D) HepG2 cells were cotransfected with the Gal4 luciferase reporter vector and with a chimera in which the Gal4 DNA binding domain is fused to the LBD of PPARγ and stimulated 18 h with rosiglitazone (Rosi, 10 μM), a PPARγ agonist, or with **1**–**11** (10 μM). Data are the mean ± SE of three experiments. $^{*}p < 0.05$ versus not treated cells (NT).

Please cite this article in press as: Renga B et al. Molecular decodification of gymnemic acids from *Gymnema sylvestre*. Discovery of a new class of liver X receptor antagonists. Steroids (2015), http://dx.doi.org/10.1016/j.steroids.2015.01.024

and PPARγ and demonstrated that gymnestrogenin (**11**) at the concentration of 50 μM failed to antagonize the transcriptional activity driven by these receptors (Fig. 5, panels A–D).

We have subsequently analyzed whether **11** regulate mRNA expression of canonical LXR target genes. As shown in Figs. 6A and B, 11 was able to reduce the expression of SREBP-1c in HepG2 cells both in basal condition and in cells co-stimulated with GW3965 as well as that of ABCA1 in THP1 cells co-stimulated with GW3965 ($p < 0.05$ versus not treated cells; $p < 0.05$ versus GW3965 stimulated cells). Furthermore, gymnestrogenin (**11**) abrogated the effects of GW3965 on intracellular lipid accumulation measured by Oil red O staining (Fig. 6C). The lipid accumulation was quantified spectrophotometrically and quantitative analysis confirmed the data to be statistically significant (Fig. 6C). Noteworthy, gymnestrogenin (**11**) was also able to reduce mRNA levels of LXRβ (Fig. 6E, $^{\#}p < 0.05$ versus GW3965 stimulated cells) but not that of LXRα (Fig. 6D) in HepG2 cells stimulated with GW3965.

Molecular modelling. Up to date, the experimental structures of ligand-LXRα,β concern small molecules acting as agonists [51–53]. In the present contribution, we proposed the first tentative model of LXRs bound to antagonists. In particular, X-ray crystallography studies show the plasticity of ligand binding domain (LBD) of LXRs [47,51–55], like many nuclear receptors [56], adapting the shape and size of binding cavity on the nature of the bound small molecule. Based on this structural consideration, we performed our analysis by using the induced fit docking protocol (IFD) [57–59] developed by Schrödinger LLC [60], which calculates movements of backbone and side chains upon ligand binding.

Our theoretical results about isoform β show that both ligands (**10** and **11**) fill equivalent spaces in the LBD of the biological target (Fig. 7A and B) presenting superimposable docked poses.

The compound **10** establishes van der Waals contacts by its polycyclic moiety and methyl groups with Ser242, Phe268, Phe271, Thr272, Leu274, Ala275, Ile277, Ser278, Ile309, Met312, Glu315, Ile327, Thr328, Phe329, Leu330, Phe340, Leu345, Phe349, His435, Gln438, Val439, Leu442, Leu449, Leu453, Trp457 (Fig. 7A). The double bond at C-12 is normal to side chain of Phe329 (Fig. 7A). The hydroxyl group at C-16 donates a hydrogen bond to the backbone CO of Met312, whereas the OH at C-21 interacts with side chain of Glu281 (Fig. 7A). The hydroxyl groups at C-23 and C-28 accept a H-bond from His435 and Thr316, respectively (Fig. 7A).

The docked pose of **11** shows the same van der Waals interactions with the residues found by **10**, (Fig. 7B), except for the further contact with Leu313. The hydrogen bonds network is also similar, but more H-bonds are observed for **11**. In particular, the hydroxyl group at C-3 accepts a hydrogen bond from side chain of Gln438 (Fig. 7B) and the OH at C-23 donates a H-bond to Gln438 (Fig. 7B). The hydroxyl group at C-21 is also hydrogen bonded to side chain of Arg319 (Fig. 7B). The superimposition of the **10** and **11** docked poses with the co-crystallized agonist of LXRβ, reveals that **10** and **11** explore different spaces of the binding site compared to the agonist (Figs. S1 and S2 in Supporting information).

Differently from the results on the isoform β, the predicted bioactive conformations of **10** and **11** are not overlapping (Fig. 8A and B) in the isoform α.

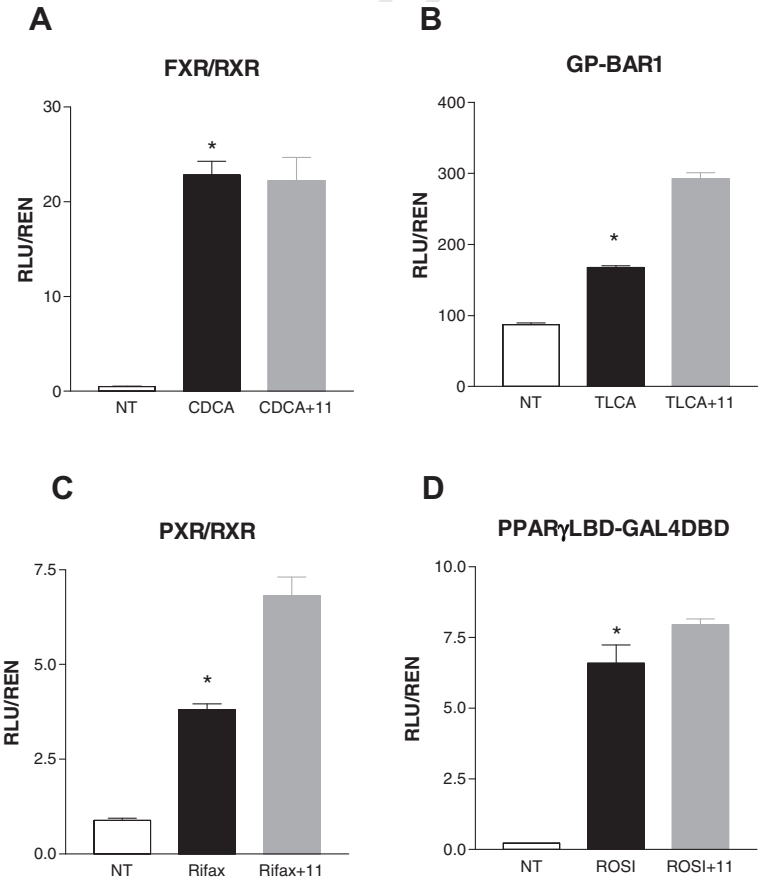

Fig. 5. Antagonism of gymnestrogenin (**11**) on other nuclear receptors. HepG2 cells (A, C and D) or HEK293T (B) cells were transfected as described in the Legend of Fig. 4. Twenty-four hour post transfection cells were stimulated with 10 μM of appropriate agonist alone or in combination with **11**, 50 μM. Data are the mean ± SE of three experiments. $^{*}p < 0.05$ versus not treated cells (NT).

Please cite this article in press as: Renga B et al. Molecular decodification of gymnemic acids from *Gymnema sylvestre*. Discovery of a new class of liver X receptor antagonists. Steroids (2015), http://dx.doi.org/10.1016/j.steroids.2015.01.024

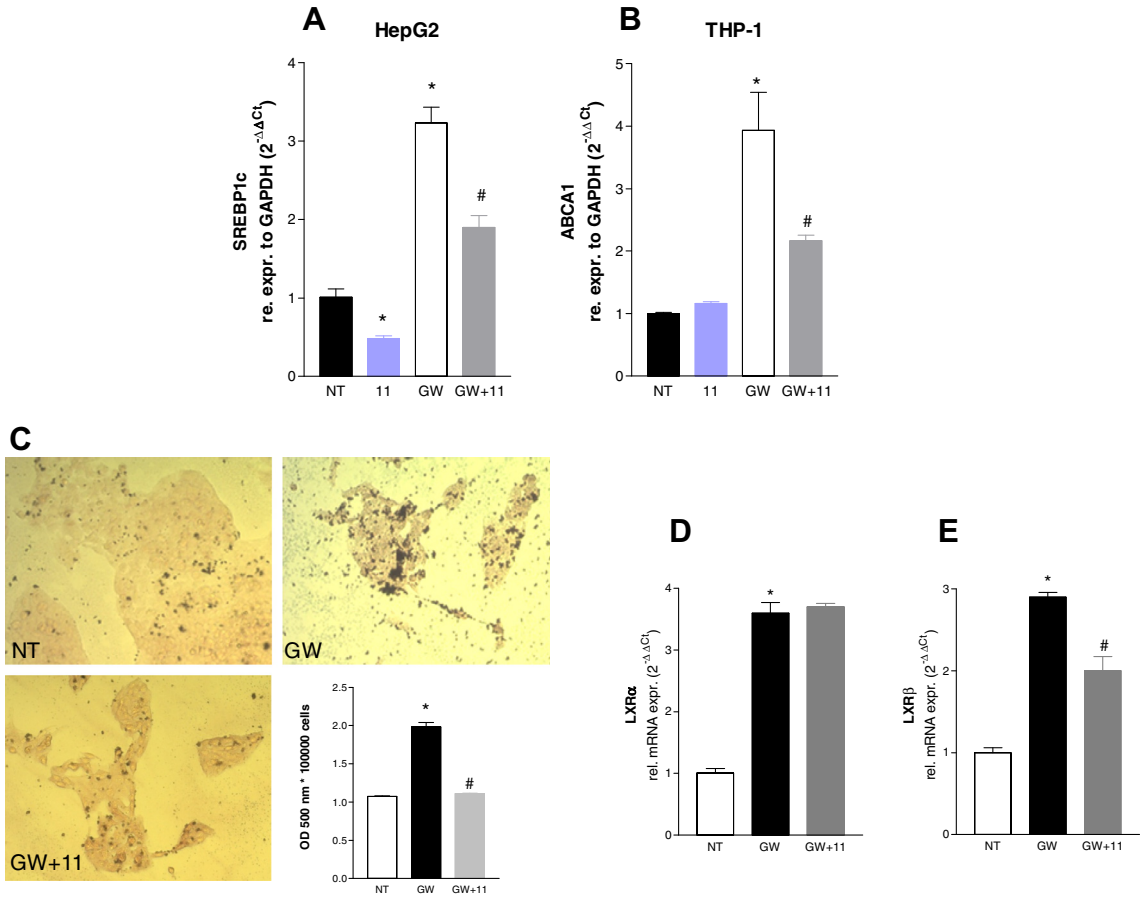

Fig. 6. Gymnestrogenin (**11**) inhibits LXR target genes and lipid accumulation in HepG2 cells. HepG2 cells (A) and THP1 (B) were incubated with **11** (10 μM), with GW3965 (10 μM) or with the combination of GW3965 and **11**. At the end of the treatment the relative mRNA expression of SREBP-1c (A) and ABCA1 (B) was assayed by Real-Time PCR. (C) Images of Oil Red O staining and Oil Red O quantification at 500 nm. (D and E) Real Time PCR analysis of mRNA expression of LXRα and LXRβ. Values are normalized relative to GAPDH mRNA and are expressed relative to those of not treated (NT) cells which are arbitrarily set to 1. GW: GW3965.

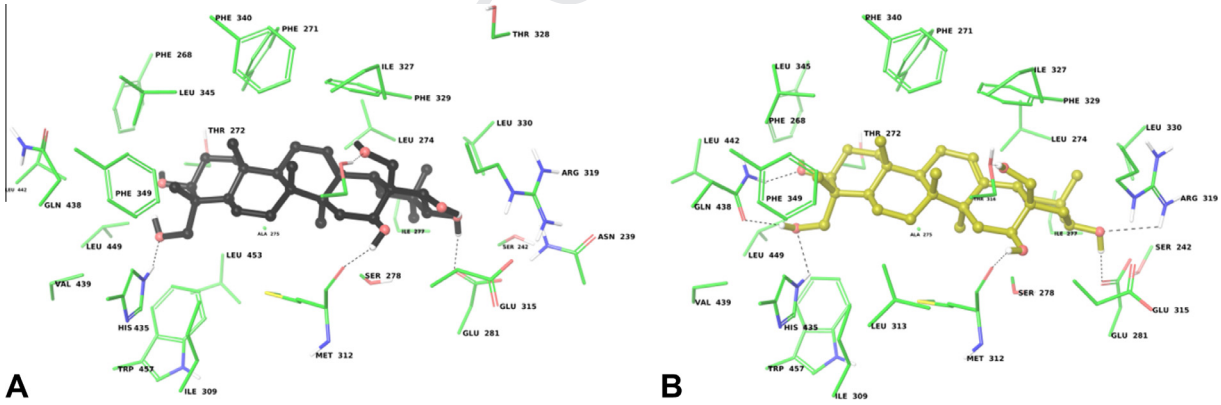

Fig. 7. (A and B) Three-dimensional models of the interactions formed by **10** (A) and **11** (B) with LXRβ. The protein is depicted by tube and coloured in green except for the following atoms: polar H, white; N, dark-blue; O, red; S, yellow. All ligands are represented by sticks (black for **10**; kaki for **11**) and balls (coloured: O, red; polar H, white). The C atoms of the small molecules are coloured as for the sticks: black for **10** and kaki for **11**. The black dashed lines indicate hydrogen bonds between protein and ligands. (For interpretation of the references to colour in this figure legend, the reader is referred to the web version of this article.)

In particular for **11**, van der Waals are observed with Phe257, Leu260, Ala261, Val263, Ser264, Met298, Leu299, Glu301, Thr302, Arg305, Ile313, Thr314, Leu316, Phe326, Leu331, Phe335, Ile339, Trp443 (Fig. 8B). In the docked pose of **11**, the double bond is parallel to the side chain of Phe315 (Fig. 8B). The OH at C-3 faces the π system of Phe326. The hydroxyl group at C-23 donates a H-bond to the backbone CO of Phe257, whereas the OH at C-28 gives the same interaction with the side chain of Glu267 (Fig. 8B). The hydroxyl groups at C-16 accepts two H-bonds from side chain of Arg232, whereas the side chain of Asn225 gives a hydrogen bond to OH at C-21 (Fig. 8B). The binding mode of **11** with LXRα presents different interactions compared to the reference agonist (Fig. S3 in Supporting information).

On the other hand, we observe that the docked pose of **10** is superimposable (Fig. S4 in Supporting information) to the co-crystallized agonist of LXRα (PDB ID: 3IPU) [51]. In fact, the presence

Please cite this article in press as: Renga B et al. Molecular decodification of gymnemic acids from *Gymnema sylvestre*. Discovery of a new class of liver X receptor antagonists. Steroids (2015), http://dx.doi.org/10.1016/j.steroids.2015.01.024

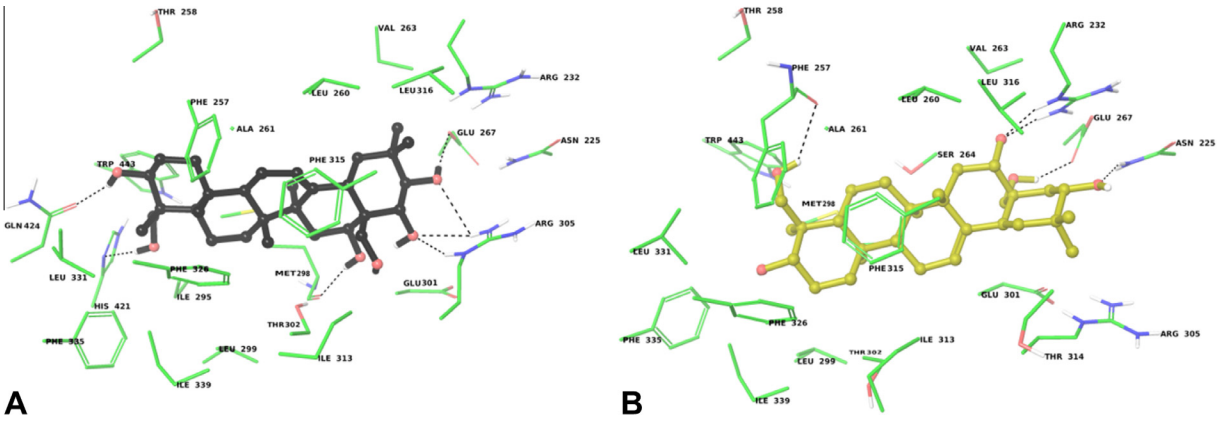

Fig. 8. (A and B) Three-dimensional models of the interactions formed by **10** (A) and **11** (B) with LXRα. The protein is depicted by tube and coloured in green except for the following atoms: polar H, white; N, dark-blue; O, red; S, yellow. All ligands are represented by sticks (black for **10**; kaki for **11**) and balls (coloured: O, red; polar H, white). The C atoms of the small molecules are coloured as for the sticks: black for **10** and kaki for **11**. The black dashed lines indicate hydrogen bonds between protein and ligands. (For interpretation of the references to colour in this figure legend, the reader is referred to the web version of this article.)

of the OH at C-22 causes the formation of two hydrogen bonds with the side chain of Arg305 (Fig. 8a), causing a relative displacement with respect to **11**. In details, in the binding cavity of LXRα, **10** is closer to the residues Asn225, Arg232, Thr258, Ser264, Ile295, Phe315, His421, Gln424 (Fig. 8A), not involved in interactions with **11**. The OH at C-3 and C-23 donate a H-bond to the side chains of Gln424 and His421, respectively (Fig. 8A). The hydroxyl group at C-16 is hydrogen bonded to backbone CO of Met298 (Fig. 8A). The OH at C-21 donates a H-bond to the side chain of Glu267 and accepts a hydrogen bonds from Arg305 (Fig. 8A).

The outcomes of both ligands against isoform β and of **11**-LXRα could suggest a perturbation of some residues in the LBD upon binding of the small molecules, negatively modulating the biological activity of the protein. Compound **10** adopts an agonist-like arrangement in the LBD of LXRα, but, as suggested from the biological experimental evidence, it is not able to interfere with the protein activity.

4. Discussion and conclusion

Fatty liver is the most common cause of asymptomatic abnormal liver function tests among adults in Western countries. Fatty liver disease affects 10–24% of the general population and 57.5–74% of obese persons [61]. The most well-known molecular pathway involved in the development of fatty liver is the activation of SREBP-1c [62]. Analysis of the mouse SREBP-1c gene promoter revealed an LXR/RXR DNA-binding site that is essential for its regulation, indicating that SREBP-1 is a direct target gene of LXR [30]. Additional support for the role of LXR came from the finding that LXR agonist treatment induces the expression of SREBP-1 target genes, such as fatty acid synthase (FAS) and increases plasma and hepatic TG levels in wild-type, but not LXR-deficient mice [31]. Consequently, LXR-null mice are defective in hepatic lipid metabolism and resistant to obesity and steatosis when challenged with a Western-style diet containing both high fat and cholesterol [63]. LXRs also contribute to the development of steatosis induced by essential polyunsaturated fatty acid deficiency [64]. Therefore, synthetic or natural compounds that inhibit LXRs activation or act as an inverse agonist for LXRs would be beneficial in patients with fatty liver disease [35,65].

In the present study we have reported the isolation and the pharmacological decodification of gymnemic acids, largely considered the active constituents of *G. sylvestre* extract. Isolated GAs and the aglycone gymnemagenin (**10**) showed the ability to selectively antagonize LXRβ in a transactivation assay in HepG2 cells transiently transfected with a chimera vector containing the LBD of LXRβ fused with the DBD of Gal4. Differently, gymnestrogenin (**11**), a less common aglycone in gymnemic acids and differing from the widespread aglycone **10** in the absence of an hydroxyl group on the ring E, was proved a potent dual LXRα/β antagonist.

Furthermore, results from our investigation have clearly demonstrated that gymnemic acids as well as gymnemagenin (**10**) and gymnestrogenin (**11**), are non promiscuous antagonists for LXRs. This specificity was confirmed by transactivation experiments. Exposure of HepG2 cells to these compounds fails to modulate the expression of a wide array of mammalian nuclear receptors and fails to activate FXR, GP-BAR1, PXR and PPARγ in transactivation assay.

Indeed analysis of transactivation assays reveals that compound **2** is the sole component of the complex mixture of GAs to be almost inactive on LXRβ when tested at 50 μM. Looking to the chemical structure of **2**, this result suggests that the presence of a D-glucuronic acid unit at C-3 with the concomitant absence of any acylating unit on the hydroxyl group around ring E is detrimental for both isoforms of LXR. On the contrary gymnemic acid VII (**1**), the corresponding 22-dehydroxyl derivative of **2**, still retains the ability to antagonize GW3965 mediated LXRβ activation thus demonstrating that the presence of the hydroxyl group at position-22 is a negative factor in the LXRβ recognition by non-acylated gymnemic acids. Otherwise the presence of acylated hydroxyl groups on ring E produces potent LXRβ antagonists independently by the chemical nature (acetyl, mba or tig), the amount (one or two) or the position (C-21, C-22 or/and C-26) of the acylating unit.

Of interest are also the results of the transactivation assays on the two aglycone moieties, gymnemagenin (**10**) and gymnestrogenin (**11**). As shown in Fig. 2B and C, the observation that gymnemagenin (**10**) retains the selective LXRβ antagonistic profile of its cognate acylated gymnemic acids (compare **10** versus compounds **3**–**9** in Fig. 2) whereas gymnestrogenin (**11**) is a dual LXRα/β antagonist points towards the profound impact engaged by position 22 in the aglycone fitting in the two LXR isoforms. Furthermore, we have shown that gymnestrogenin (**11**) failed to antagonize other nuclear receptors as well as that the antagonism potency on LXRα and β occurred with an IC_{50} of 2.5 μM and 1.4 μM respectively, thus representing a promising template in generating selective dual LXRα/β antagonists.

In this study we have further investigated the effects of **11** in modulating LXRs target genes by RT-PCR. Using HepG2 cells we have shown that gymnestrogenin (**11**) reduces the expression of SREBP1c, a transcription factor that promotes the expression of

lipogenic genes, a typical effect of LXR activation in the liver. Similarly, we have shown that gymnestrogenin (**11**) is able in antagonizing the LXR mediated induction of ABCA1 in THP1 cells. ABCA1 is a transporter that mediates cholesterol efflux from lipid laden macrophages onto HDL particles for transport back to the liver. Thus, gymnestrogenin (**11**) was able to reduce lipid accumulation in HepG2 cells. Indeed, morphological observation and quantitative analysis have demonstrated that intracellular lipid content increased after treatment of cells with GW3965 while co-administration of both LXR agonist and gymnestrogenin significantly reduced red lipid droplets inside cells. Finally, another important finding we made in this study was that **11** retains the ability to reduce the relative mRNA expression of LXRβ but not that of LXRα. The slight repressive effect of **11** on the expression of LXRβ might be explained by the following: (i) gymnestrogenin (**11**) is a more potent antagonist of LXRβ (IC_{50} of 1.4 μM) instead of LXRα (IC_{50} of 2.5 μM); (ii) the promoter of LXRs contains multiple LXRE that allow to the autoregulation of LXR gene expression following interaction with agonists/antagonists [66]. Thus, gymnestrogenin (**11**) could reduce the transcriptional activity of LXR even on its own promoter, thus reducing the mRNA expression.

The results of this study, along with the well demonstrate hydrolytic biotransformation of gymnemic acids to corresponding aglycones in the gastrointestinal tract after oral administration [67] substantiate the use of *G. sylvestre* extract in LXR mediated dislypidemic diseases.

Appendix A. Supplementary data

Supplementary data associated with this article can be found, in the online version, at http://dx.doi.org/10.1016/j.steroids.2015.01.024.

References

[1] Kapoor LD. Handbook of ayurvedic medicinal plants. Boca Raton, FL: CRC Press; 1990. p. 200.
[2] Kanetkar P, Singhal R, Kamat M. *Gymnema sylvestre*: a memoir. J Clin Biochem Nutr 2005;1:77–81.
[3] Saneja A, Sharma C, Aneja KR, Pahwa R. *Gymnema Sylvestre* (Gurmar): a review. Der Pharmacia Lettre 2010;2:275–84.
[4] Porchezhian E, Dobriyal RM. An overview on the advances of *Gymnema sylvestre*: chemistry, pharmacology and patents. Pharmazie 2003;58:5–12.
[5] Shigematsu N, Asano R, Shimosaka M, Okazaki M. Effect of administration with the extract of *Gymnema sylvestre* R. Br. leaves on lipid metabolism in rats. Biol Pharm Bull 2001;24:713–7.
[6] Persaud SJ, Majed HA, Raman A, Jones PM. *Gymnema sylvestre* stimulates insulin release in vitro by increased membrane permeability. J Endocrinol 1999;163:207–12.
[7] Shanmugasundaram ERB, Gopinath KL, Shanmugasundaram KR, Rajendran VM. Possible regeneration of the islets of Langerhans in streptozocin-diabetic rats given *Gymnema sylvestre* leaf extracts. J Ethnopharmacol 1990;30:265–79.
[8] Baskaran K, Ahamath BK, Shanmugasundaram KR, Shanmugasundaram ERB. Antidiabetic effect of a leaf extract from *Gymnema sylvestre* in noninsulin dependent diabetes mellitus patients. J Ethnopharmacol 1990;30:295–305.
[9] Tiwari P, Mishra BN, Sangwan NS. Phytochemical and pharmacological properties of *Gymnema sylvestre*: an important medicinal plant. Biomed Res Int 2014. http://dx.doi.org/10.1155/2014/830285.
[10] Di Fabio G, Romanucci V, De Marco A, Zarrelli A. Triterpenoids from *Gymnema sylvestre* and their pharmacological activities. Molecules 2014;19:10956–81.
[11] Patil AN, Nirmal SA, Chavan AK. Development and validation of HPTLC method for estimation of gymnemic acid in microencapsulated antidiabetic polyherbal formulations. Acta Chromatogr 2013;25:601–12.
[12] Wang Y, Dawid C, Kottra G, Daniel H, Hofmann T. Gymnemic acids inhibit sodium-dependent glucose transporter. J Agric Food Chem 2014;62:5925–31.
[13] Preuss HG, Bagchi D, Bagchi M, Rao CV, Dey DK, et al. Effects of a natural extract of (−)-hydroxycitric acid (HCA-SX) and a combination of HCA-SX plus niacin-bound chromium and *Gymnema sylvestre* extract on weight loss. Diabetes Obes Metab 2004;6:171–80.
[14] Bishayee A, Chatterjee M. Hypolipidemic and antiatherosclerotic effects of *Gymnema sylvestre* leaf extract in albino rats fed on high fat diet. Phys Res 1994;8:118–20.
[15] Kalaany NY, Mangelsdorf DJ. LXRs and FXR: the yin and yang of cholesterol and fat metabolism. Annu Rev Physiol 2006;68:159–91.
[16] Tontonoz P, Mangelsdorf DJ. Liver X receptor signaling pathways in cardiovascular disease. Mol Endocrinol 2003;17:985–93.
[17] Swanson HI, Wada T, Xie W, Renga B, Zampella A, et al. Role of nuclear receptors in lipid dysfunction and obesity-related diseases. Drug Metab Dispos 2013;41:1–11.
[18] Janowski BA, Willy PJ, Devi TR, Falck JR, Mangelsdorf DJ. An oxysterol signalling pathway mediated by the nuclear receptor LXR alpha. Nature 1996; 383:728–31.
[19] Lehmann JM, Kliewer SA, Moore LB, Smith-Oliver TA, Oliver BB, et al. Activation of the nuclear receptor LXR by oxysterols defines a new hormone response pathway. J Biol Chem 1997;272:3137–40.
[20] Venkateswaran A, Laffitte BA, Joseph SB, Mak PA, Wilpitz DC, et al. Control of cellular cholesterol efflux by the nuclear oxysterol receptor LXR alpha. Proc Natl Acad Sci USA 2000;97:12097–102.
[21] Chawla A, Boisvert WA, Lee CH, Laffitte BA, Barak Y, et al. A PPAR gamma-LXR-ABCA1 pathway in macrophages is involved in cholesterol efflux and atherogenesis. Mol Cell 2001;7:161–71.
[22] Costet P, Luo Y, Wang N, Tall AR. Sterol-dependent transactivation of the ABC1 promoter by the liver X receptor/retinoid X receptor. J Biol Chem 2000;275: 28240–5.
[23] Laffitte BA, Repa JJ, Joseph SB, Wilpitz DC, Kast HR, et al. LXRs control lipid-inducible expression of the apolipoprotein E gene in macrophages and adipocytes. Proc Natl Acad Sci USA 2001;98:507–12.
[24] Repa JJ, Turley SD, Lobaccaro JA, Medina J, Li L, et al. Regulation of absorption and ABC1-mediated efflux of cholesterol by RXR heterodimers. Science 2000;289:1524–9.
[25] Joseph SB, Bradley MN, Castrillo A, Bruhn KW, Mak PA, Pei L, et al. LXR-dependent gene expression is important for macrophage survival and the innate immune response. Cell 2004;119:299–309.
[26] A-Gonzalez N, Bensinger SJ, Hong C, Beceiro S, Bradley MN. Apoptotic cells promote their own clearance and immune tolerance through activation of the nuclear receptor LXR. Immunity 2009;31:245–58.
[27] Laffitte BA, Chao LC, Li J, Walczak R, Hummasti S, et al. Activation of liver X receptor improves glucose tolerance through coordinate regulation of glucose metabolism in liver and adipose tissue. Proc Natl Acad Sci USA 2003;100: 5419–24.
[28] Commerford SR, Vargas L, Dorfman SE, Mitro N, Rocheford EC, et al. Dissection of the insulin-sensitizing effect of liver X receptor ligands. Mol Endocrinol 2007;21:3002–12.
[29] Loren J, Huang Z, Laffitte BA, Molteni V. Liver X receptor modulators: a review of recently patented compounds (2009–2012). Expert Opin Ther Pat 2013;23: 1317–35.
[30] Schultz JR, Tu H, Luk A, Repa JJ, Medina JC, et al. Role of LXRs in control of lipogenesis. Genes Dev 2000;14:2831–8.
[31] Repa JJ, Liang G, Ou J, Bashmakov Y, Lobaccaro JM, et al. Regulation of mouse sterol regulatory element-binding protein-1c gene (SREBP-1c) by oxysterol receptors, LXRalpha and LXRbeta. Genes Dev 2000;14:2819–30.
[32] Joseph SB, Laffitte BA, Patel PH, Watson MA, Matsukuma KE, et al. Direct and indirect mechanisms for regulation of fatty acid synthase gene expression by liver X receptors. J Biol Chem 2002;277:11019–25.
[33] Grefhorst A, Elzinga BM, Voshol PJ, Plösch T, Kok T, et al. Stimulation of lipogenesis by pharmacological activation of the liver X receptor leads to production of large, triglyceride-rich very low density lipoprotein particles. J Biol Chem 2002;277:34182–90.
[34] Sim WC, Park S, Lee KY, Je YT, Yin HQ, et al. LXR-α antagonist meso-dihydroguaiaretic acid attenuates high-fat diet-induced nonalcoholic fatty liver. Biochem Pharmacol 2014;90:414–24.
[35] Griffett K, Solt LA, El-Gendy Bel-D, Kamenecka TM, et al. A liver-selective LXR inverse agonist that suppresses hepatic steatosis. ACS Chem Biol 2013;8: 559–67.
[36] D'Auria MV, Sepe V, Zampella A. Natural ligands for nuclear receptors: biology and potential therapeutic applications. Curr Top Med Chem 2012;12:637–69.
[37] Fiorucci S, Distrutti E, Bifulco G, D'Auria MV, Zampella A. Marine sponge steroids as nuclear receptor ligands. Trends Pharmacol Sci 2012;33:591–601.
[38] Liu HM, Kiuchi F, Tsuda Y. Isolation and structure elucidation of gymnemic acids, antisweet principles of *Gymnema sylvestre*. Chem Pharm Bull 1992;40: 1366–75.
[39] Kazujo Y, Kayoko A, Shigenobu A, Kouji M. Gymenmic acids V, VI and VII from Gur-ma, the leaves of *Gymnema sylvestre* R. Br.. Chem Pharm Bull 1989;37: 852–4.
[40] Yoshikawa K, Amimoto K, Arihara S, Matsuura K. Structure studies of new antisweet constituents from *Gymnema sylvestre*. Tetrahedron Lett 1989;30: 1103–6.
[41] Yoshikawa K, Nakagawa M, Yamamoto R, Arihara S, Matsuura K. Antisweet natural products. V. Structures of gymnemic acids VIII–XII from *Gymnema sylvestre* R. Br.. Chem Pharm Bull 1992;40:1779–82.
[42] Schrödinger Release 2013–3: MacroModel, version 10.2, Schrödinger, LLC, New York, NY, 2013.
[43] Halgren TA. Merck molecular force field. V. Extension of MMFF94 using experimental data, additional computational data, and empirical rules. J Comput Chem 1996;17:616–41.
[44] Still WC, Tempczyk A, Hawley RC, Hendrickson T. The GB/SA continuum model for solvation. A fast analytical method for the calculation of approximate born radii. J Am Chem Soc 1990;112:6127–9.
[45] www.rcsb.org.

[46] Berman HM, Westbrook J, Feng Z, Gilliland G, Bhat TN, et al. The protein data bank. Nucleic Acids Res 2000;28:235–42.
[47] Zuercher WJ, Buckholz RG, Campobasso N, Collins JL, Galardi CM, et al. Discovery of tertiary sulfonamides as potent liver X receptor antagonists. J Med Chem 2010;53:3412–6.
[48] Sastry GM, Adzhigirey M, Day T, Annabhimoju R, Sherman W. Protein and ligand preparation: parameters, protocols, and influence on virtual screening enrichments. J Comput Aid Mol Des 2013;27:221–34.
[49] Schrödinger Release 2013–3: Schrödinger Suite 2013 Protein Preparation Wizard; Epik version 2.6, Schrödinger, LLC, New York, NY, 2013; Impact version 6.1, Schrödinger, LLC, New York, NY, 2013; Prime version 3.3, Schrödinger, LLC, New York, NY, 2013.
[50] Genet C, Strehle A, Schmidt C, Boudjelal G, Lobstein A, et al. Structure-Activity relationship study of betulinic acid, a novel and selective TGR5 agonist, and its synthetic derivatives: potential impact in diabetes. J Med Chem 2010;53:178–90.
[51] Fradera X, Vu D, Nimz O, Skene R, Hosfield D, et al. X-ray structures of the LXRα LBD in its homodimeric form and implications for heterodimer signaling. J Mol Biol 2010;399:120–32.
[52] Jaye MC, Krawiec JA, Campobasso N, Smallwood A, Qiu C, et al. Discovery of substituted maleimides as liver X receptor agonists and determination of a ligand-bound crystal structure. J Med Chem 2005;48:5419–22.
[53] Svensson S, Ostberg T, Jacobsson M, Norström C, Stefansson K, et al. Crystal structure of the heterodimeric complex of LXRalpha and RXRbeta ligand-binding domains in a fully agonistic conformation. EMBO J 2003;22:4625–33.
[54] Farnegardh M, Bonn T, Sun S, Ljunggren J, Ahola H, et al. The three-dimensional structure of the liver X receptor beta reveals a flexible ligand-binding pocket that can accommodate fundamentally different ligands. J Biol Chem 2003;278:38821–8.
[55] Hoerer S, Schmid A, Heckel A, Budzinski RM, Nar H. Crystal structure of the human liver X receptor beta ligand-binding domain in complex with a synthetic agonist. J Mol Biol 2003;334:853–61.
[56] Di Micco S, Renga B, Carino A, D'Auria MV, Zampella A, et al. Structural insights into estrogen related receptor-β modulation: 4-methylenesterols from *Theonella swinhoei* sponge as the first example of marine natural antagonists. Steroids 2014;80:51–63.
[57] Farid R, Day T, Friesner RA, Pearlstein RA. New insights about HERG blockade obtained from protein modeling, potential energy mapping, and docking studies. Bioorg Med Chem 2006;14:3160–73.
[58] Sherman W, Day T, Jacobson MP, Friesner RA, Farid R. Novel procedure for modeling ligand/receptor induced fit effects. J Med Chem 2006;49:534–53.
[59] Sherman W, Beard HS, Farid R. Use of an induced fit receptor structure in virtual screening. Chem Biol Drug Des 2006;67:83–4.
[60] Small-Molecule Drug Discovery Suite 2013–3: Schrödinger Suite 2013–3 Induced Fit Docking protocol; Glide version 6.1, Schrödinger, LLC, New York, NY, 2013; Prime version 3.4, Schrödinger, LLC, New York, NY, 2013.
[61] Angulo P. Nonalcoholic fatty liver disease. N Engl J Med 2002;346:1221–31.
[62] Zhou G, Myers R, Li Y, Chen Y, Shen X, et al. Role of AMPactivated protein kinase in mechanism of metformin action. J Clin Invest 2001;108:1167–74.
[63] Kalaany NY, Gauthier KC, Zavacki AM, Mammen PP, Kitazume T, Peterson JA, et al. LXRs regulate the balance between fat storage and oxidation. Cell Metab 2005;1:231–44.
[64] Ducheix S, Montagner A, Polizzi A, Lasserre F, Marmugi A, et al. Essential fatty acids deficiency promotes lipogenic gene expression and hepatic steatosis through the liver X receptor. J Hepatol 2013;58:984–92.
[65] Hwahng SH, Ki SH, Bae EJ, Kim HE, Kim SG. Role of adenosine monophosphateactivated protein kinase-p70 ribosomal S6 kinase-1 pathway in repression of liver X receptor-alpha-dependent lipogenic gene induction and hepatic steatosis by a novel class of dithiolethiones. Hepatology 2009;49:1913–25.
[66] Laffitte BA, Joseph SB, Walczak R, Pei L, Wilpitz DC, et al. Autoregulation of the human liver X receptor alpha promoter. Mol Cell Biol 2001;22:7558–68.
[67] Kamble B, Gupta A, Patil D, Khatal L, Janrao S, et al. Determination of gymnemagenin in rat plasma using high-performance liquid chromatography-tandem mass spectrometry: application to pharmacokinetics after oral administration of *Gymnema sylvestre* extract. Biomed Chromatogr 2013;27:669–75.

Please cite this article in press as: Renga B et al. Molecular decodification of gymnemic acids from *Gymnema sylvestre*. Discovery of a new class of liver X receptor antagonists. Steroids (2015), http://dx.doi.org/10.1016/j.steroids.2015.01.024